Effect of Surrogate Model on Screening-based Simulated Annealing for OPR-1000 Loading Pattern Optimization

Seongjin Jeong (*Presenter*), Hyun Chul Lee *(Advisor)*

Transactions of the Korean Nuclear Society Spring Meeting
May 07, 2026

Nuclear System Division, School of Mechanical Engineering
Pusan National University

Reactor Physics Lab. (RPL)

부산대학교 기계공학부
PUSAN NATIONAL UNIVERSITY
SCHOOL OF MECHANICAL ENGINEERING

Outline

1. Introduction

2. Methodology
   - Surrogate Models
   - Predictive Performance
   - Optimization Setup

3. Results

4. Conclusions

Introduction

Research Background

➢ Loading pattern (LP) optimization

- Extends cycle length while satisfying design limits.
- Direct evaluation of numerous candidates is impractical.
  - Large combinatorial search space.
  - High computational cost of 3D core analyses.

➢ Simulated Annealing (SA)[1]

- Effective for discrete optimization problems.
- Probabilistic acceptance rule enables extensive exploration.
- Promotes convergence as annealing schedule proceeds.

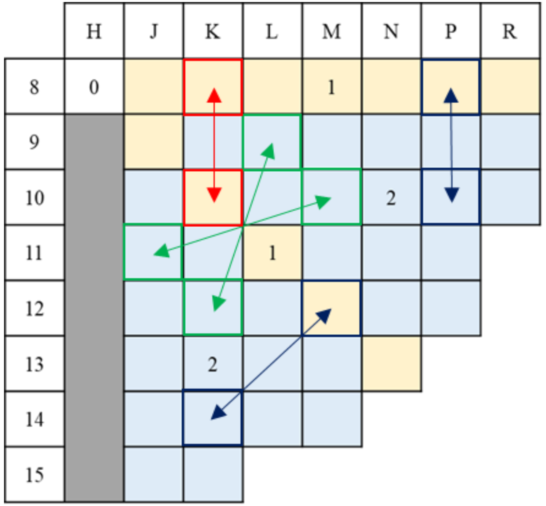

Example of FA shuffling for a new LP.

[1] D. J. Kropaczek and P. J. Turinsky, In-Core Nuclear Fuel Management Optimization for Pressurized Water Reactor Using Simulated Annealing, Nuclear Technology, 95(1), 9-32 (1991).

Previous Research – Surrogate-assisted SA

➢ Surrogate-assisted SA Framework

- Screen candidate LPs with fast surrogate predictions.
- 3D core calculations for uncertain cases or when all targets are improved over the reference.
- Reduce expensive evaluations while maintaining physics verification.

➢ Screening efficiency

- Ratio of surrogate-evaluated candidates to total evaluations.

$$Screening\ efficiency = \frac{Surrogate\ prediction}{3D\ core\ calculation + Surrogate\ prediction}$$

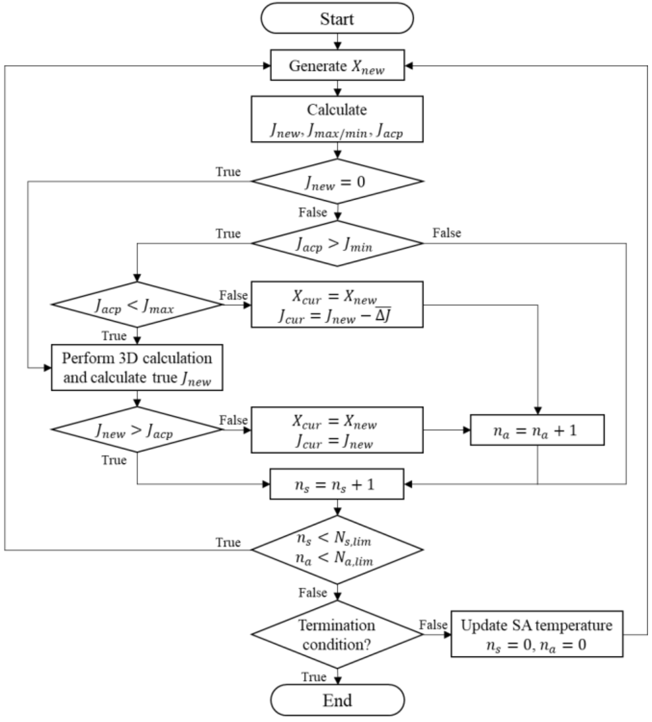

Flow chart of surrogate-assisted SA with screening technique.

[2] T.K. Park, H.G. Joo, C.H. Kim, and H.C. Lee, Multiobjective Loading Pattern Optimization by Simulated Annealing Employing Discontinuous Penalty Function and Screening Technique, Nuclear Science and Engineering, 162(2), 134–147 (2009).

Research Objective

➢ Objective

- Investigate how surrogate model characteristics affect the behavior and outcomes of screening-based SA for OPR-1000 LP optimization under identical settings.

➢ Surrogates compared

- Assembly-wise CNN[3]
  - Assembly-level input resolution
  - Local feature extraction (Convolution layer)
- Pin-wise ViT[4]
  - Pin-level input resolution
  - Global attention (Transformer encoder layer)

➢ Evaluation items

- Predictive performance
- Screening efficiency & computational cost
- Optimization reliability

Input of the assembly-wise CNN

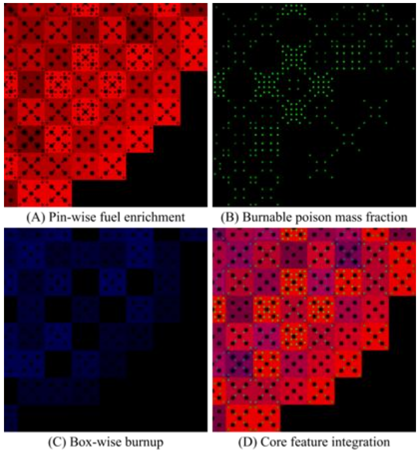

Input of the pin-wise ViT

[3] H. Jang, H.C. Lee, and H.C. Shin, Refinement of convolutional neural network for neutronic design parameter prediction of a loading pattern, RPHA 2019, 175–178 (2019).
[4] S. Jeong and H. C. Lee, Loading Pattern Optimization for OPR-1000 by Adaptive Simulated Annealing with a Screening Technique using Pin-wise Vision Transformer, RPHA 2025, (2025).

Methodology

Surrogate Models (1/2) – Assembly-wise CNN

Model Input

- 8×8 FA lattice → 4-channel 3D tensor
- Channels
  - Assembly-averaged enrichment (wt.% ^{235}U)
  - No. of burnable poison (BP) rods (#)
  - BP mass fraction (wt.% Gd_2O_3)
  - Assembly-wise burnup (MWd/kgU)

Architecture

- Convolution blocks
  - Learn spatial correlations among neighboring assemblies.
- Regression head
  - Outputs cycle length & max-F_{xy} predictions.

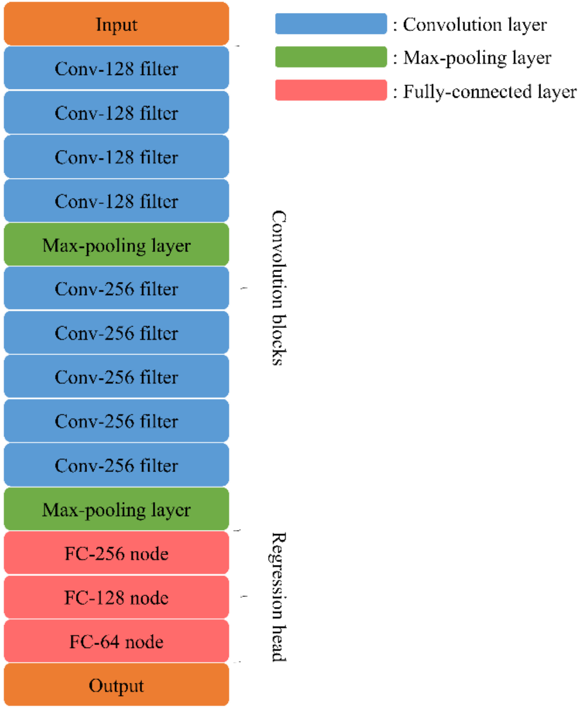

Architecture of the assembly-wise CNN

[3] H. Jang, H.C. Lee, and H.C. Shin, Refinement of convolutional neural network for neutronic design parameter prediction of a loading pattern, RPHA 2019, 175–178 (2019).

Surrogate Models (2/2) – Pin-wise ViT

➢ Model Input

- 120×120 pin lattice → 3-channel 3D tensor
- Channels
  - Pin enrichment (wt.% ^{235}U)
  - BP mass fraction (wt.% Gd_2O_3)
  - Box-wise burnup (MWd/kgU)
    - Constant value assigned per quarter assembly.

➢ Architecture

- Patch embeddings
  - Divide input tensor into fixed-size patches.
- Transformer encoder
  - Learn global interactions across patches.
- Multi-layer perceptron
  - Outputs cycle length & max-F_{xy} predictions.

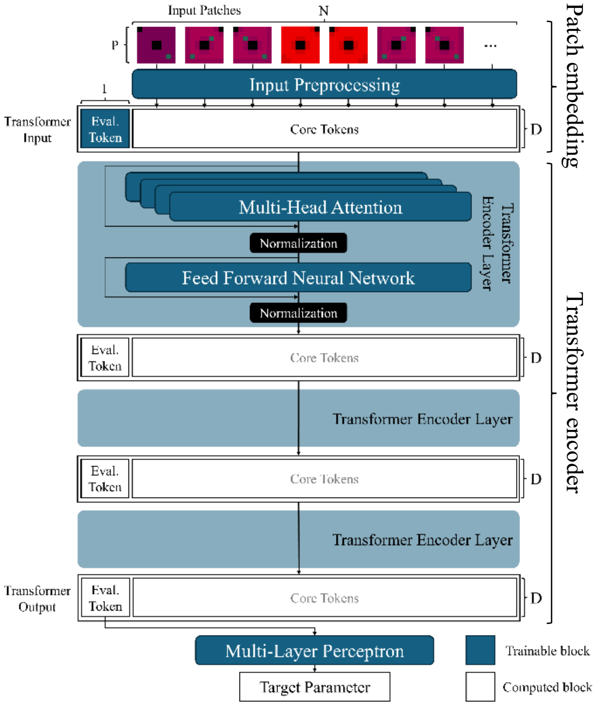

Architecture of the pin-wise ViT

[4] S. Jeong and H. C. Lee, Loading Pattern Optimization for OPR-1000 by Adaptive Simulated Annealing with a Screening Technique using Pin-wise Vision Transformer, RPHA 2025, (2025).

Predictive Performance (1/2)

➢ Training and validation datasets[4]

- Random generation (RG)
  - FA shuffles based on NDR core.
    → Covers a broad region of the search space.
- Near optimal (NO)
  - SA performed with RG-trained model.
    → Focuses on high-quality LP region.
- External validation (EV)
  - Replace one FA type in the RG + NO dataset with an unseen type.
  - Not used in training, tests generalization to unseen FA types.

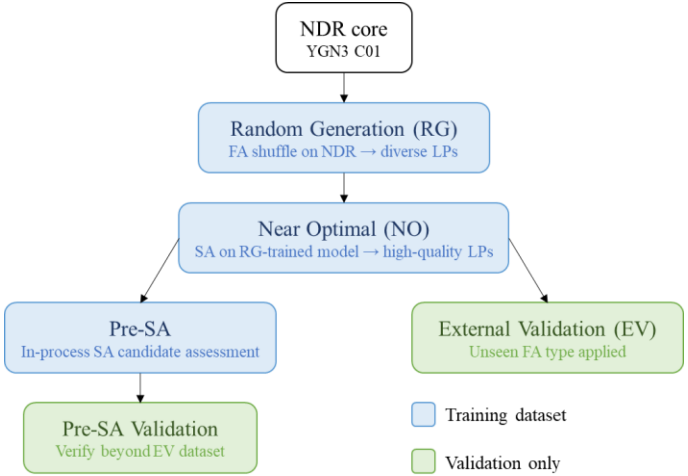

Overview of training and validation dataset construction.

➢ Pre-SA dataset

- Candidate LPs from SA process using RG+NO-trained model.
- Verifies prediction accuracy for LPs beyond EV dataset.

[4] S. Jeong and H. C. Lee, Loading Pattern Optimization for OPR-1000 by Adaptive Simulated Annealing with a Screening Technique using Pin-wise Vision Transformer, RPHA 2025, (2025).

Predictive Performance (2/2)

➢ Additional training with pre-SA candidates

- Outliers observed in max-F_{xy} predictions for pre-SA candidates.
  - MaxARE[2)] was 53.6% for assembly-wise CNN and 37.6% for pin-wise ViT.
- Max-F_{xy} prediction models were additionally trained on 90% of pre-SA candidates.
  - Remaining 10% reserved for validation.

➢ Predictive performance

Error metric	Cycle length		Max-F_{xy}	
	Assembly-wise CNN	Pin-wise ViT	Assembly-wise CNN	Pin-wise ViT
RMSRE[1)] (%)	0.94	0.16	8.19	0.86
MaxARE[2)] (%)	10.0	0.90	40.5	0.99

1) RMSRE: Root mean square value of relative error.
2) MaxARE: Maximum value of absolute relative error.

SA Optimization Setup (1/2)

➢ Optimization constraint

- Fixing-type: total No. of FAs per type fixed throughout optimization.
  - Candidates generated by positional shuffling only.
- Eliminates FA composition changes → isolates surrogate effect on SA.
- Optimization targets: longer cycle length and lower max-F_{xy} than NDR core values.

➢ SA algorithm

- Multi-objective adaptive SA[2,5]
  - Objective function: $J(X) = \sum_{i\in\{cycle\ length, max-F_{xy}\}} \left(1 + \frac{\delta_i(X)^2}{\delta_i^2}\right) u(\delta_i(X))$
    - $J(X) = 0$ if all targets improved; penalized otherwise.
  - Annealing schedule adaptively determined from candidate LP distribution.
- Screening Technique
  - When acceptance criterion is outside surrogate uncertainty range → directly accept/reject.
  - Uncertain cases or both targets improved over the reference → 3D core calculation.

[2] T.K. Park, H.G. Joo, C.H. Kim, and H.C. Lee, Multiobjective Loading Pattern Optimization by Simulated Annealing Employing Discontinuous Penalty Function and Screening Technique, Nuclear Science and Engineering, 162(2), 134–147 (2009).
[5] H.C. Lee, H.J. Shim, and C.H. Kim, “Parallel Computing Adaptive Simulated Annealing Scheme for Fuel Assembly Loading Pattern Optimization in PWR’s,” Nuclear Technology, 125(1), 39-50 (2001).

SA Optimization Setup (2/2)

➢ Target core: Hanbit Unit 3 Cycle 1 (YGN3 C01) NDR core

- Fuel assembly types in the target core[6]

Name	Enrichment (wt.% ^{235}U)		No. of rods (Zoned / BP)	BP fraction (wt.% Gd_2O_3)	No. of FAs	Name	Enrichment (wt.% ^{235}U)		No. of rods (Zoned / BP)	BP fraction (wt.% Gd_2O_3)	No. of FAs
	Normal	Zoned					Normal	Zoned			
A0	1.30	-	- / -	-	45	C1	2.87	2.36	52 / 8	4.0	32
B0	2.37	-	- / -	-	20	D0	3.35	2.87	52 / -	-	12
B1	2.36	1.30	52 / 8	4.0	8	D1	3.36	2.85	52 / 8	4.0	8
B2	2.37	-	- / 4	4.0	16	D2	3.35	2.87	100 / 8	4.0	24
C0	2.87	2.35	52 / -	-	12	-					

➢ Experimental design

- 10 independent SA runs per surrogate under identical settings.
  - Evaluates optimization reliability across 10 independent SA runs.

[6] S.K. Lee, et al., Nuclear Design Report for Yonggwang Nuclear Power Plant Unit 3 Cycle 1, Korea Atomic Energy Research Institute (1995).

Results

Results (1/3) – Assembly-wise CNN Performance

➢ Screening performance

- Screening efficiency: 89 – 91% across 10 runs.
- ~10× reduction in CPU time vs. estimated time without screening.

Metric	3D core calculation (#)	Surrogate prediction (#)	Screening efficiency (%)	CPU time (h)	Est. CPU time w/o screening (h)	Cycle length (EFPDs)	Max-F_{xy} (-)
Average	2,753	25,110	90.1	230.1	2,321.9	374.4	1.5388

➢ Optimization outcomes

- 2 of 10 runs failed to satisfy max-F_{xy} constraint.
- Representative optimal LP (run 7): (cycle length) 374.8 EFPDs, (max-Fxy) 1.5402.

SA runs	1	2	3	4	5	6	**7**	8	9	10	**NDR**
Cycle length (EFPDs)	374.5	374.8	373.5	373.8	373.7	374.5	**374.8**	374.6	374.5	373.5	**373.2**
Max-F_{xy} (-)	1.5254	**1.5423**	1.5396	1.5378	1.539	1.5388	**1.5402**	**1.5468**	1.5388	1.5391	**1.5412**

Results (2/3) – Pin-wise ViT Performance

➢ Screening performance

- Screening efficiency: 99.9% across 10 runs.
- ~750× reduction in CPU time vs. estimated time without screening.

Metric	3D core calculation (#)	Surrogate prediction (#)	Screening efficiency (%)	CPU time (h)	Est. CPU time w/o screening (h)	Cycle length (EFPDs)	Max-F_{xy} (-)
Average	23	22,738	99.9	2.5	1,896.7	374.5	1.5261

➢ Optimization outcomes

- All 10 runs satisfied constraints.
- Representative optimal LP (run 3): (cycle length) 375.1 EFPDs, (max-Fxy) 1.4965.

SA runs	1	2	**3**	4	5	6	7	8	9	10	**NDR**
Cycle length (EFPDs)	373.9	374.7	**375.1**	374.4	373.9	374.4	374.7	374.5	374.4	375.1	**373.2**
Max-F_{xy} (-)	1.5351	1.5276	**1.4965**	1.5347	1.5351	1.5347	1.5276	1.5388	1.5347	1.4965	**1.5412**

Results (3/3) – Optimal LP Comparison

➢ NDR core and representative optimal LPs

	H	J	K	L	M	N	P	R
8	A0	B1	B2	A0	B2	B1	C1	D0
9		B0	A0	D2	A0	B2	C1	C0
10		A0	C1	A0	C1	A0	D2	B0
11		D2	A0	C1	A0	D2	D0	
12		A0	C1	A0	C1	D1	B0	
13		B2	A0	D2	D1	C0		
14		C1	D2	D0	B0			
15		C0	B0					

NDR core

	H	J	K	L	M	N	P	R
8	A0	B1	C0	B0	A0	C1	B2	B2
9		C1	A0	C1	A0	B2	D2	D1
10		A0	B1	A0	D2	D2	A0	B0
11		C1	A0	C1	A0	C1	D0	
12		A0	D2	A0	C1	C0	B0	
13		B2	D2	C1	C0	D0		
14		D2	A0	D0	B0			
15		D1	B0					

Assembly-wise CNN (run 07)

	H	J	K	L	M	N	P	R
8	A0	B1	B2	A0	B1	B2	C1	D0
9		B0	A0	D2	A0	C1	B2	C0
10		A0	C1	A0	C1	A0	D2	B0
11		D2	A0	C1	A0	D2	D0	
12		A0	C1	A0	C1	D1	B0	
13		C1	A0	D2	D1	C0		
14		B2	D2	D0	B0			
15		C0	B0					

Pin-wise ViT (run 03)

Conclusions

Conclusions

➢ Predictive performance

- Outliers in pre-SA candidate predictions were reduced after additional training.
- RMSRE of pin-wise ViT was ~5× lower than that of assembly-wise CNN.

➢ Optimization results

Metric	Assembly-wise CNN	Pin-wise ViT
Screening efficiency	~90%	~99.9%
3D core calculations	~2,750 per run	~28 per run
CPU time	150 – 300 h	2 – 4 h
Optimization success	8 / 10	10 / 10

Impact of Surrogate Characteristics

➢ Assembly-wise CNN

- Lower input resolution limits max-F_{xy} prediction precision.
- Residual bias creates artificial barriers/wells in SA search.
  - Requires more stages and evaluations.
- 2 of 10 runs failed to satisfy max-F_{xy} constraint.

➢ Pin-wise ViT

- Pin-level resolution supports precise max-F_{xy} prediction.
  - A more stable surrogate landscape enables consistent SA convergence.
- All 10 runs satisfied constraints within hours.

Input resolution and prediction precision are critical for optimization reliability and efficiency.

Future Work

- **Detailed analysis of surrogate uncertainty and bias**
  - Assess how surrogate uncertainty distorts the SA search trajectory.
  - Develop strategies to reduce prediction bias and outliers in assembly-wise CNN.
- **LP optimization via reinforcement learning (RL)**
  - Leverage ViT surrogate for fast LP evaluations.
  - Explore policy/value-based approaches as alternatives to SA.

References

1. D. J. Kropaczek and P. J. Turinsky, In-Core Nuclear Fuel Management Optimization for Pressurized Water Reactor Using Simulated Annealing, Nuclear Technology, 95(1), 9-32 (1991).
2. T.K. Park, H.G. Joo, C.H. Kim, and H.C. Lee, Multiobjective Loading Pattern Optimization by Simulated Annealing Employing Discontinuous Penalty Function and Screening Technique, Nuclear Science and Engineering, 162(2), 134–147 (2009).
3. H. Jang, H.C. Lee, and H.C. Shin, Refinement of convolutional neural network for neutronic design parameter prediction of a loading pattern, RPHA 2019, 175–178 (2019).
4. S. Jeong and H. C. Lee, Loading Pattern Optimization for OPR-1000 by Adaptive Simulated Annealing with a Screening Technique using Pin-wise Vision Transformer, RPHA 2025, (2025).
5. H.C. Lee, H.J. Shim, and C.H. Kim, "Parallel Computing Adaptive Simulated Annealing Scheme for Fuel Assembly Loading Pattern Optimization in PWR's," Nuclear Technology, 125(1), 39-50 (2001).
6. S.K. Lee, et al., Nuclear Design Report for Yonggwang Nuclear Power Plant Unit 3 Cycle 1, Korea Atomic Energy Research Institute (1995).

Appendix A. SA Results with Assembly-wise CNN

➤ Evaluation counts and screening efficiency using the assembly-wise CNN.

SA runs	3D core calculation (#)	Surrogate prediction (#)	Screening efficiency (%)	CPU time (h)	Est. CPU time w/o screening (h)	Cycle length (EFPDs)	Max-F_{xy} (-)
1	2,902	28,012	90.6	242.6	2,576.2	374.5	1.5254
2	2,754	22,358	89.0	230.1	2,092.7	374.8	**1.5423**
3	3,135	32,187	91.1	262.1	2,943.5	373.5	1.5396
4	2,355	20,292	89.6	196.8	1,887.3	373.8	1.5378
5	1,795	17,845	90.9	150.1	1,636.7	373.7	1.5390
6	3,321	29,061	89.7	277.6	2,698.5	374.5	1.5388
7	2,825	27,604	90.7	236.2	2,535.8	374.8	1.5402
8	3,515	32,023	90.1	293.8	2,961.5	374.6	**1.5468**
9	2,252	18,344	89.1	188.2	1,716.3	374.5	1.5388
10	2,675	23,378	89.7	223.6	2,171.1	373.5	1.5391
Average	2,753	25,110	90.1	230.1	2,321.9	374.4	1.5388

Appendix B. SA Results with Pin-wise ViT

➢ Evaluation counts and screening efficiency using the pin-wise ViT.

SA runs	3D core calculation (#)	Surrogate prediction (#)	Screening efficiency (%)	CPU time (h)	Est. CPU time w/o screening (h)	Cycle length (EFPDs)	Max-F_{xy} (-)
1	24	23,684	99.9	2.7	1,975.7	373.9	1.5351
2	22	22,278	99.9	2.5	1,858.3	374.7	1.5276
3	22	22,377	99.9	2.5	1,866.6	375.1	1.4965
4	22	22,276	99.9	2.5	1,858.2	374.4	1.5347
5	23	23,071	99.9	2.6	1,924.5	373.9	1.5351
6	23	23,047	99.9	2.6	1,922.5	374.4	1.5347
7	19	20,214	99.9	2.1	1,686.1	374.7	1.5276
8	24	23,695	99.9	2.7	1,976.6	374.4	1.5347
9	23	22,976	99.9	2.6	1,916.6	374.4	1.5347
10	24	23,757	99.9	2.7	1,981.8	375.1	1.4965
Average	23	22,738	99.9	2.5	1,896.7	374.5	1.5257